Published in final edited form as:
J Comp Neurol. 2010 February 15; 518(4): 526–546. doi:10.1002/cne.22236.

Neurogenin1 effectively reprograms cultured chick RPE cells to differentiate towards photoreceptors

Run-Tao Yan[1], **Lina Liang**[1,2], **Wenxin Ma**[1], **Xiumei Li**[1], **Wenlian Xie**[1,3], and **Shu-Zhen Wang**[1]

[1]Department of Ophthalmology, University of Alabama at Birmingham, Birmingham, Alabama, USA

Abstract

Photoreceptors are highly specialized sensory neurons in the retina, and their degeneration results in blindness. Replacement with developing photoreceptor cells promises to be an effective therapy, but it requires a supply of new photoreceptors, because the neural retina in human eyes lacks regeneration capability. We report efficient generation of differentiating, photoreceptor-like neurons from chick retinal pigment epithelial (RPE) cells propagated in culture through reprogramming with *neurogenin*1 (*ngn1*). In reprogrammed culture, a large number of the cells (85.0 ± 5.9%) began to differentiate towards photoreceptors. Reprogrammed cells expressed transcription factors that set in motion photoreceptor differentiation, including Crx, Nr2E3, NeuroD, and RXRγ, and phototransduction pathway components, including transducin, cGMP-gated channel, and red opsin of cone photoreceptors (equivalent to rhodopsin of rod photoreceptors). They developed inner segments rich in mitochondria. Furthermore, they responded to light by decreasing their cellular free calcium (Ca^{2+}) levels and responded to 9-cis-retinal by increasing their Ca^{2+} levels after photobleaching, hallmarks of photoreceptor physiology. The high efficiency and the advanced photoreceptor differentiation indicate *ngn1* as a gene of choice to reprogram RPE progeny cells to differentiate into photoreceptor neurons in future cell replacement studies.

Keywords

retina; reprogramming; Ca^{2+} imaging; light response

Introduction

Photoreceptors in the vertebrate retina are specialized primary neurons that are responsible for initiating the visual process. Upon capturing photons, photoreceptors generate electrophysiological signals that are modulated and transmitted to the brain through secondary neurons of the retina. Like other neurons, photoreceptors are terminally differentiated and do not re-enter the cell cycle for regeneration. Thus, photoreceptors that die due to various causes cannot be replenished, leading to irreversible vision loss. The importance of vision to quality of life has spurred a spectrum of investigations ranging from photoreceptor rescue (for review, see Adler et. al., 1999; Lavail, 2001; Bennett, 2004) to cell

Correspondence: S-Z Wang, 700 South 18th Street, Birmingham, AL 35294-0009. Tel: (205) 325-8628; Fax: (205) 325-8679; szwang@uab.edu.
[2]Current address: Eye Hospital, China Academy of Chinese Medical Sciences, Beijing, China
[3]Current address: Sun Yat-sen University, Guangzhou, China

Commercial relationships: None.

replacement by retinal regeneration (Otteson, 2003; Raymond, 1991; Stenkamp and Cameron, 2002) or by cell transplantation (Aramant and Seiler, 2002; Young, 2005). Replacement through transplantation of developing photoreceptor cells has been shown to be effective in restoring vision in blind mice (MacLaren et al., 2006). This promising intervention presents a need for a source of new photoreceptors (Bennett, 2007).

Cells of the retinal pigment epithelial (RPE) could be a potential source of photoreceptor cells. Unlike retinal neurons, RPE cells from many species, including mouse, rat, and human, can re-enter the cell cycle to proliferate. Further, the progeny cells may adopt a fate other than RPE. For example, embryonic chick and rodent RPE can be stimulated by basic-fibroblast growth factor to transdifferentiate into a neural retina (Park and Hollenberg, 1989; Pittack et al., 1991; Zhao et al., 1995; Sakami et al., 2008). However, employing this "RPE → neural retina" transdifferentiation mechanism for photoreceptor production remains challenging, because the process does not occur with dissociated cells nor in embryos older than day 4.5 (E4.5) in chick or E13 in rodents (Pittack et al., 1991; Zhao et al., 1995; Sakami et al., 2008).

A different approach has been taken to guide RPE to give rise to photoreceptor cells. A key component of this approach is to initiate photoreceptor differentiation with regulatory genes playing instrumental roles in retinal photoreceptor production. Previous studies showed that RPE progeny cells can differentiate towards photoreceptors when guided by *ash1*, *ath5*, *neuroD*, and *ngn2*, genes homologous to Drosophila proneural genes and encoding transcription factors in the basic Helix-Loop-Helix (bHLH) family. Nonetheless, photoreceptor-like cells are present in small numbers and do not represent the major product of programming by *ash1* (Mao et al., 2008) or by *ath5* (Ma et al., 2004; Xie et al., 2004). The yield improves with *ngn2*, but significant amount of other types of retinal cells are also generated (Yan et al., 2001). In *neuroD*-reprogrammed culture, photoreceptor-like cells are the major products (Yan and Wang, 1998), and they closely resemble developing photoreceptors at the molecular, cellular, and physiological levels (Yan and Wang, 2000b; Liang et al., 2008). When grafted into embryonic chick eyes, the cells migrate into the photoreceptor layer and emanate axonal arborization into the outer plexiform layer (Liang et al., 2006). An issue remains, though, that the yield is rather low: less than 30% of the total cells in *neuroD*-reprogrammed cultures display signs of photoreceptor differentiation (Liang et al., 2008). This low efficiency could be related to *neuroD*'s function in the retina. In the retina, *neuroD* promotes the differentiation and the survival of photoreceptors (Yan and Wang, 1998; 2004; Pennesi et al., 2003; Liu et al., 2008). Theoretically, a gene upstream of *neuroD* and able to steer multipotent progenitor cells to the photoreceptor path would be a better choice to reprogram RPE for photoreceptor production. A search for such an upstream gene has recently identified *ngn1* (Yan et al., submitted), a member of the *neurogenin* subfamily of bHLH genes with proneural activities.

In this study, we tested *ngn1's* ability to reprogram cultured chick RPE cells to differentiate towards photoreceptor cells. We report efficient generation of photoreceptor-like neurons with *ngn1*, outperforming *neuroD* and *ngn2*. Further analyses at the molecular, cellular, and physiological levels showed that *ngn1*-reprogrammed cells expressed an array of photoreceptor genes and exhibited photoreceptor morphologies. Physiologically, they responded to light by decreasing their cellular free calcium (Ca^{2+}) levels. Further, light-bleached, reprogrammed cells responded to 9-cis-retinal by increasing Ca^{2+} levels, reminiscent of visual recovery. Our results indicate *ngn1* as a gene of choice to reprogram RPE progeny cells to differentiate towards photoreceptors.

Materials and Methods

Chick embryos

Fertilized, pathogen-free White Leghorn chicken (*Gallus gallus*) eggs were purchased from Spafas and incubated in a Petersime incubator. All use of animals adhered to the procedures and policies set by the Institutional Animal Use and Care Committee at the University of Alabama at Birmingham (UAB).

Generation of retroviruses

Replication Competent Avian Splice (RCAS) retrovirus (Hughes et al., 1987) was used to drive the expression of genes in cultured RPE cells. The coding sequences of homeodomain genes *chx10* (NCBI accession # AF178671), *crx* (NCBI accession # AF28517), *pax6* (NCBI accession # NM_205066), *rax*/rx (NCBI accession # AB015750), *raxL* (AF420601), *six3* (NCBI accession # AY373324), and *six9* (NCBI accession # AJ011786), and proneural bHLH gene *ath3* (NCBI accession # Y09597) were RT-PCR amplified based on publicly available sequence information. After cloning into pGEM-T and sequence verification, the coding region of each gene was subcloned into RCAS, via shuttle vector Cla12Nco (Hughes et al., 1987). To rule out frame-shift or stop mutations, recombinant RCAS proviral DNA was sequenced at the UAB Genomics Core Facility. All recombinant DNA procedures followed the National Institutes of Health guidelines. Recombinant RCAS proviral DNA was transfected into chick embryonic fibroblast cells for the production of viral particles, as previously described (Yan and Wang, 1998). RCAS expressing *ash1* (Mao et al., 2009), *ath5* (Ma et al., 2004), *NSCL1* (Li et al., 1999), *NSCL2* (Li et al., 2001), *neuroD* (Yan and Wang, 1998), *ngn1* (Yan et al., submitted), *ngn2* (Yan et al., 2001), *ngn3* (Ma et al., 2009), and *sox2* (Ma et al., 2009) were produced as described. The titers of concentrated viral stocks ranged 1 - 3 × 10^8 pfu/ml.

RPE cell culture

Primary RPE cell culture was established with RPE isolated from E6 and E15 chick eyes after dissociation with trypsin/EDTA and gentle trituration (Yan and Wang, 1998). An equivalent of 1/3 of an E6 RPE (or 1/5 of an E15 RPE) was seeded in a 35-mm culture dish for a density that covered roughly 5% of the surface. Cells were cultured with Knockout D-MEM supplemented with 20% serum replacement (Invitrogen). For experiments with trophic factors, dissociated RPE cells were cultured in the presence of 10 - 20 ng/ml of brain-derived neurotrophic factor (BDNF; Sigma), ciliary neurotrophic factor (CNTF; Sigma), basic FGF (bFGF; Sigma), glia derived neurotrophic factor (GDNF; Sigma), and nerve growth factor (NGF; Sigma). Otherwise, dissociated RPE cells were first cultured for 3 - 4 days to reach approximately 50% confluence. At this point, 10 - 20 μl of concentrated recombinant RCAS retrovirus was added to each culture dish. RCAS-GFP (Yan and Wang, 1998) was used as a negative control. Cultures were maintained for an additional 10 - 12 days with Medium 199 (M199) supplemented with 10% fetal calf serum (FCS) changed every other day. Cells were subjected to Ca^{2+} imaging, or they were fixed for immunostaining, in situ hybridization, or electron microscopy.

Retinal cell culture

E16 (and E18) retinas were isolated and their cells were dissociated with trypsin/EDTA. Dissociated retinal cells were seeded onto polyornithine-treated substratum, cultured for 6 days with M199 plus 10% FCS.

Antibody characterization

Please see Table 1 for a list of all antibodies used.

Rabbit polyclonal antibody against AP2 recognized AP-2α and, to a lesser extent, AP-2β and AP-2γ of AP2 proteins (Data Sheet from Santa Cruz Biotechnology). The antibody specifically recognized a 50 kDa protein (corresponding to AP2α) on a Western blot of nuclear extract from Hela cells engineered to express AP2α. Immunohistochemical analyses of the chick retina carried out in different laboratories (including our own) show that the antibody specifically labels amacrine and horizontal cells, with all other cell types being immuno-negative (Bisgrove and Godbout, 1999; Li et al., 2001; Mao et al., 2009). A mouse monoclonal antibody against AP2α (clone 3B5) also specifically labels amacrine and horizontal cells in the chick retina (Bisgrove and Godbout, 1999; Li et al., 2001; Fisher et al., 2007; Mao et al., 2009; Ma et al., 2009). Monoclonal antibody against Brn3A specifically recognized Brn3A, with no reactivity to Brn3B or Brn3C by Western blots and, and showed no reactivity to Brn3A knockout mice (Data Sheet from Chemicon/Millipore). In the mammalian retina, the anti-Brn3A antibody specifically labels ganglion cells, with all other retinal cells being immuno-negative (Xiang et al., 1995). Consistent with the results, our experiments using the chick retina showed specific labeling of retinal ganglion cells by the anti-Brn3A antibody (Ma et al., 2009; Mao et al., 2009). Rabbit polyclonal antibody against calretinin recognized a 29 kDa protein that corresponded to calretinin (Data Sheet from Chemicon/Millipore). The antibody reacted with both the calcium-bound and calcium-unbound conformations of calretinin. In retinal sections, the antibody labels amacrine, ganglion, and horizontal cells, but not other cells (Ellis et al., 1991; Fischer et al., 2007). Monoclonal antibody against Islet-1 recognized a 36 kDa protein (corresponding to Islet-1) on a Western blot (Data Sheet from the Developmental Studies Hybridoma Bank (DSHB; Iowa University). In the retinal sections, the antibody identifies ganglion cells during early phase of chick retinal development (Austin et al., 1995; Li et al., 2001; Ma et al., 2009) and subsequently also in bipolar cells (our unpublished observation). Monoclonal antibody against LIM recognizes both LIM 1 and LIM 2 proteins (Data Sheet from DSHB). Examination of retinal sections by others (Liu et al., 2000) and our laboratory (Li et al., 2001; Mao et al., 2009; Ma et al., 2009) showed that the antibody recognizes specifically horizontal cells, with all other cells in the retina lacking immunostaining. Preparation of affinity purified rabbit polyclonal antibody against chick NeuroD and its specificity have been previously described (Yan and Wang, 2004). In essence, Western blot analysis showed that the anti-NeuroD antibody recognized a single protein band of 40 kDa (corresponding to the NeuroD protein) of nuclear extracts of the chick retinal cells, and no reactivity was observed in the control (nuclear extract of heart cells). Immunocytochemical analysis gave showed specific, nuclear staining of RPE cells transduced to express *neuroD*, but not in control RPE cells. Immunohistochemistry gave a staining pattern consistent with the pattern delineated with in situ hybridization. Rabbit polyclonal antibody against red opsin recognized red/green opsin with band of ~40 kDa, but not blue and other opsins (Data Sheet from Chemicon/Millipore). In the rabbit (MacNeil and Gaul, 2008) and the chick (Liang et al., 2009) retina, the antibody labels cone photoreceptors specifically, while cells of all other types lack immunostaining signals. Polyclonal antibody against RCAS viral protein p27 specifically recognized the viral protein (27 kDa; Data Sheet from Spafas). The antibody produces immunostaining in chick tissues and cells infection by RCAS virus, but gives no staining in tissues and cells lacking the viral infection (Yan and Wang, 1998; 2004; Li et al., 2001; Ma et al., 2009; Mao et al., 2009). Monoclonal antibody against Pax6 identifies predominantly amacrine cells, along with progenitor cells and ganglion cells in the chick retina (Belecky-Adams et al., 1997; Fischer et al., 2007). Generated from immunizing mouse with E10 tectal homogenate, monoclonal antibody RA4 recognizes a microtubule associated protein of long-projecting axons (Mcloon and Barnes, 1989). The antibody recognized only a 140 kDa protein with no additional RA-4-positive bands detected in Western blots of cell lysates prepared from retinas at various stages, from E4 to adult. In immunostaining of chick retinal sections, RA-4 specifically labels ganglion cells, particularly their axons, and does not label other types of cells (Waid and McLoon, 1995).

This pattern of staining has also been observed in our studies (Ma et al., 2009). Monoclonal antibody against vimentin recognized chick vimentin (52 kDa; Data Sheet from DSHB) and labels Muller glia in the chick retina (Hunt and Davis, 1990; Herman et al., 1993; Li et al., 2001). Anti-visinin labels predominantly photoreceptor cells and, to a much less extent, some cells in the amacrine cell layer in the developing chick retina (Hatakenaka et al., 1985; Yan and Wang, 1998; 2004; Mao et al., 2009).

Immunocytochemistry

Cells in culture were fixed with ice-cold 4% paraformaldehyde in PBS (pH 7.4) for 30 minutes at room temperature and subjected to standard immunocytochemistry with primary antibodies listed in Table 1 and described in the previous paragraph and with alkaline phosphatase-, horseradish peroxidase- (Vector Laboratories), or fluorophore-conjugated (Molecular Probes) secondary antibodies, following the procedures provided by the manufacturers.

In situ hybridization

Sequences (500-800 base pairs) corresponding to the C' region of Crx, RXRγ (NCBI accession # X58997), Nr2e3 (NCBI accession # NM-204594), and RaxL were PCR amplified from chick retinal cDNA. PCR products were cloned into pGEM-T. All cloned DNAs were sequenced for verification. Linearized plasmids harboring the sequences were used to synthesize digoxigenin (dig)-labeled antisense RNA probes using the Genius kit (Roche Molecular Biochemicals) following the manufacturer's instructions. Dig-labeled antisense RNA probes against the cone type α-subunit of transducin (ALT), the α-subunit of cone cGMP-gated channel (CNGA3), and the α-subunit of rod cGMP-gated channel (CNGA1) were prepared as described (Liang et al., 2008). In situ hybridization was carried out as previously described (Yan and Wang, 2000b).

Statistical analysis

Cell numbers were counted under a 40 x objective for samples with a large number positive of cells, or under a 20 x objective when the fewer positive cells were present. The cell numbers under different magnifications were normalized to an area of 242 mm^2. The means and SDs of the numbers from at least 3 independent images were calculated using Origin 7.0 (OriginLab Corp.). One-way ANOVA of Origin 7.0 was used for statistical significance analysis at 0.05 (*) and 0.01 (**) levels.

Electron microscopy

E17 chick eye and RPE cell cultures were processed as described (Liang et al., 2008). Ultrathin sections (70-90 nm thick) were examined with a JEOL 1200 EX II transmission electron microscope.

Calcium imaging of light response

Calcium imaging of cells in culture was carried out using Fluo-4 AM (Molecular Probes), as previously described (Liang et al., 2008). Briefly, the cells were dark adapted overnight and incubated with Fluo-4 AM (4 μM in M199), followed by fluorescent photomicrography under a 40x objective using a Nikon TE300 inverted microscope equipped with a 100 W-HBO mercury light source. Images were captured with a Q-Imaging MicroPublisher 5.0 digital camera (2-s exposure) using a filter set with maximal excitation of 488 nm and emission at 517 nm. For light response, an image was captured before subjecting the cells to visible light. After the initial image was captured, cells in the dish were subjected to visible light (set at the maximum) on the microscope for various lengths of time. Immediately following the light exposure, another fluorescent image was captured. All steps were

performed with room lights off. To quantify fluorescent intensity, the integrated optical density (IOD) was measured using LabWorks™ (version 4.0, UVP Inc.). The means and SDs of IODs from 3-15 cells in one or more images were calculated with Origin 7.0.

For molecular identification after Ca^{2+} imaging, cells were fixed with 4% paraformaldehyde and subjected to immunostaining with specific antibodies against photoreceptor proteins visinin and red opsin. For experiments with CNG channel blockers, cells were incubated with Fluo-4 AM as described above, and then incubated with 2 ml of M199 containing 3 μM each of dichlorobenzamil and l-cis-diltiazem (Sigma). They were then subjected to light exposure and imaging, as described above.

Calcium imaging of responses to 9-cis-retinal

Cells in a primary RPE cell culture infected with RCAS-ngn1 were trypsinized and reseeded onto polyornithine-treated coverslips at low density to obtain isolated cells. The reseeded cells were incubated with Fluo-4 AM. After 1-3 min of light exposure, the cells were subjected to either vehicle control (50 μl of 1:100 dilution of DMSO with M199), 9-cis-retinal (50 μl of 0.5 mM in M199; stock solution: 50 mM in DMSO), or sequentially with vehicle control first and then 9-cis-retinal after replacement of the solution in the dish (to minimize changes in DMSO concentration). Images were captured at various time points.

Photomicrograph production

Results of immunocytochemistry and in situ hybridization were captured with Q-Imaging MicroPublisher 5.0 digital camera attached to the Nikon TE300 inverted microscope, and the images were saved without modification. For production of photomicrographs, the data were retrieved with Adobe Photoshop (San Jose, CA) and corrected for brightness and contrast with Photoshop. For photomicrographs on calcium imaging, data images were retrieved with Photoshop and corrected for brightness and contrast at the same degree (a fixed setting) with the program.

Results

Massive amount of visinin$^+$ cells in *ngn1*-reprogrammed RPE cell culture

We first used E6 chick RPE cell cultures to test *ngn1's* ability to reprogram the otherwise non-neural RPE cells propagated in culture to differentiate towards photoreceptors. The RPE cells were dissociated and seeded at a density covering about 5% of the culture substratum. Replication-competent retrovirus RCAS expressing *ngn1* (RCAS-ngn1) was added to the culture when it reached ~50% confluency. The culture was later examined for the presence of photoreceptor-like cells with commensurate morphologies and the expression of visinin, a calcium-binding protein present in cone photoreceptors (Yamagata et al., 1990), which are the dominant photoreceptor type in the chick retina.

During the initial culture period, RPE cells proliferate and lose their dark pigmentation. As the culture ages and become confluent (~ 9 days), RPE cells become re-pigmented (Liang et al., 2006). Morphologically, chick RPE cells in culture display hexagonal or fibroblast-like appearances and form monolayer upon confluency (Liang et al., 2006; Fig. 1A). However, cultures infected with RCAS-ngn1 contained large numbers of clusters (aggregates) of cells with compact cell bodies and processes (Fig. 1B), characteristic of development photoreceptor neurons in culture. Cells in the clusters remained un-pigmented. A previous RT-PCR analysis has shown that infection of E6 RPE cell culture with RCAS-ngn1 represses the expression of *mmp115* and *mitf*, genes important to maintaining RPE properties (Li et al., 2009). The clusters, along with cells displaying neuron-like morphologies but in isolation, emerged 4 days after the addition of RCAS-ngn1. During the

initial 4 days, cells with neuron-like morphologies were scarce, likely due to that it takes a few days for the culture to become thoroughly infected by RCAS (Yan and Wang, 1998) and that expression of a transgene from the virus becomes apparent 21-24 hours after infection (Reddy et al., 1991; Fekete and Cepko, 1993). Scoring the numbers of cells in the clusters against the total in five view areas showed that those neuron-like cells accounted for 82.2 ± 4.1% of the total present. As the culture aged, the clusters enlarged, and those cells that maintained RPE-like eventually covered the remaining surface of the culture dish. Immunostaining showed massive amount of visinin$^+$ cells, some of which showed weaker staining than the rest (Fig. 1C). Cell clustering and the weak staining made it difficult to score the exact number of visinin$^+$ cells in large clusters. Scoring cell numbers in 8 view areas at places with small clusters and individual cells showed that visinin$^+$ cells accounted for 85.0 ± 5.9% of the total cells present. In sharp contrast to the hexagonal RPE cells, visinin$^+$ cells resembled photoreceptors, with an elongated cell body, an axon-like process, an inner segment-like compartment, and a structural feature reminiscent of the lipid droplet (Fig. 1D,E).

To comparatively analyze *ngn1*'s efficiency and to search for an optimal molecular trigger to induce RPE cells to differentiate towards photoreceptors, we assayed additional regulatory genes shown or implicated to be important for retinal progenitor and/or photoreceptor development, along with 5 neurotrophic factors (BDNF, CNTF, bFGF, GDNF, and NGF). These regulatory genes included (i) those known to be important for retinal progenitor cells: *sox2* (Taranova et al., 2006), *chx10* (Burmeister et al., 1996), *pax6* (Marquardt et al., 2001), *rax/rx* (Mathers and Jamrich, 2000), *six3* (Zhu et al., 2002), and *six6/six9/Optx2* (Toy et al., 1998); and (ii) those shown to be essential for photoreceptor development: *crx* (Chen et at., 1997; Furukawa et al., 1997) and *raxL* (Chen and Cepko, 2002). For comparison, we included proneural bHLH genes involved in retinal neurogenesis: *ash1* (Tomita et al., 1996), *ath3* (Tomita et al., 2000), *ath5* (Brown et al., 1998; Wang et al., 2001), *NSCL1* (Li et al., 1999), *NSCL2* (Li et al., 2001), *neuroD* (Yan and Wang, 1998; Pennesi et al., 2003; Liu et al., 2008), and *ngn2* (Marquardt et al., 2001; Yan et al., 2001), and *ngn3* (Ma et al., 2009), the third member of the *neurogenin* family. As previously reported, visinin$^+$ cells were absent in RPE cell culture infected with RCAS-GFP (Yan and Wang, 1998; Fig. 2A) but were present in cultures infected with RCAS-ash1 (Mao et al., 2009), RCAS-ath5 (Ma et al., 2004; Fig. 2B), RCAS-neuroD (Yan and Wang, 1998; Fig. 2C), or RCAS-ngn2 (Yan et al., 2001; Fig. 2D). Cultures infected with RCAS-ngn3 gave rise to large numbers of visinin$^+$ cells (Fig. 2E), similar to that with RCAS-ngn1 (Fig. 2F). Cell number scoring showed that *ngn1* induced the highest number of visinin$^+$ cells (Fig. 2I). Comparatively, the number of visinin$^+$ cells in *ash1*- or *ath5*-reprogramed culture was <2% of that in *ngn1*-reprogramed culture (Fig. 2J). In *neuroD*- or *ngn2*-reprogramed cultures, the number of visinin$^+$ cells was ~20 and 30%, respectively, of that in *ngn1*-reprogramed culture. The number of visinin$^+$ cells in *ngn3*-reprogramed cultures was ~82% of that in *ngn1*-reprogramed culture. Nonetheless, the difference in the number of visinin$^+$ cells between *ngn1* and *ngn3* was not statistically significant ($p=2.03$), while the two genes induced significantly ($p<0.01$) higher numbers of visinin$^+$ cells than did *ash1*, *ath5*, *neuroD*, and *ngn2*. Overall, there seemed an order of *ngn1* ≈ *ngn3* > *ngn2* > *neuroD* > *ash1* > *ath5*. No visinin$^+$ cells were produced by treatment with the growth factors or by the rest of the regulatory genes included in the test (data not shown).

We then tested RPE cell cultures derived from embryos at day 15, when the RPE is molecularly and physiologically close to maturity (Rizzolo et al., 2007). *Ngn1* outperformed *ngn2* and induced more visinin$^+$ cells (Fig. 2G,H). On the other hand, *neuroD* became ineffective with few visinin$^+$ cells generated (data not shown). Thus, *ngn1* remained as the frontrunner in inducing E15 RPE cells to differentiate towards photoreceptor cells.

Expression of photoreceptor genes

Because visinin expression alone does not necessarily reflect an RPE → photoreceptor reprogramming event, RPE cell cultures infected with RCAS-ngn1 were examined for the expression of photoreceptor genes. For differentiation, photoreceptors employ transcriptional factors that set in motion their differentiation program. Key regulators include *crx* (Chen et al., 1997; Furukawa et al., 1997), *neuroD* (Yan and Wang, 1998; Yan and Wang, 2004; Liu et al., 2008), *nr2e3* (Mears et al., 2001; Milam et al., 2002), *raxL* (Chen and Cepko, 2002), and *RXRγ* (Roberts et al., 2005). Immunostaining with a specific antibody against NeuroD showed a large number of cells (271,752 ± 38,834 per 242 mm^2) to be immuno-positive (Fig. 3A; Table 2). In situ hybridization and RT-PCR detected the induction of *RXRγ* (Fig. 3B), *crx* (Fig. 3C,D), *raxL* (Fig. 3E,Q), and *nr2e3* (Fig. 3Q).

Photoreceptors are highly specialized cells devoted to capturing photons and initiating the visual pathway. For their unique functions, photoreceptors synthesize a set of specific proteins that participate in the phototransduction pathway, converting light into electro-physiological signals. To determine whether the reprogrammed cells could be capable of phototransduction, we examined the expression of additional phototransduction components (besides visinin). Immunocytochemistry with a specific antibody against red opsin showed immunopositive cells in the reprogrammed culture (Fig. 3F-N), but not in the control (data not shown). The sub-cellular patterns of red opsin immunostaining were of two types. One was the immunostaining as dot-like (Fig. 3G, arrowhead), similar to anti-red opsin immunostaining observed with the retina, in which red opsin localizes to the outer segment. Under a 100x objective, the dots appeared to be cellular apices (Fig. 3K-N, arrowhead). Double immunostaining showed red opsin at the apices of some individual visinin$^+$ cells (Fig. 3O, inset). The other type was immunostaining of the cytoplasmic compartment (Fig. 3F,H-J, O), a deviation from the typical localization of red opsin in intact, mature photoreceptors. This mis-localization of opsin is not unexpected, because studies have shown similar mis-localization when retinal photoreceptors are separated from their native environment (Bok, 1993). In a reseeded culture, red opsin$^+$ cells displayed cellular compartments resembling a membranous expansion at the tip (Fig. 3H-J, arrowhead) and an elongated inner-segment. Expression of the α-subunits of cone (A3) and rod (A1) CNG channels (Fig. 3P) and cone α-transducin (Fig. 3Q) were also detected in the reprogrammed culture. Compared with visinin, an early marker for cone differentiation, genes associated with advanced differentiation were expressed in fewer cells in the reprogrammed cultures (Table 2). This is attributed to the restrictive effects of culture conditions on photoreceptor differentiation and maturation. Previously experiments with RPE explants show that prolonging culture period to 16 day results in red opsin$^+$ cells accounting for >50% of visinin$^+$ cells (Li et al., 2009). In the chick retina, red cones predominate cone population, which accounts for >90% of photoreceptors.

Next, we examined the reprogrammed culture for the expression of markers that identify other types of retinal cells. We found a small number of calretinin$^+$ cells (Fig. 4B; Table 2), which in the retina include horizontal, amacrine, and ganglion cells. The number of calretinin$^+$ cells was very low, 5,203 ± 960 per 242 mm^2 and equaling <2% of visinin$^+$ cells (Table 2). Double labeling showed that a few visinin$^+$ cells were calretinin$^+$ (Fig. 4A,B). Notably, some of the calretinin$^+$ cells exhibited typical photoreceptor morphologies with a lipid-droplet-like structure (Fig. 4C,D). It is unclear whether these double-labeled cells represent “mixed” cell type, or a transient stage in their differentiation and maturation. A small number of RA4$^+$ cells (524 ± 185 per 242 mm^2 and equivalent to 0.2% of visinin$^+$ cells) were present in reprogrammed cultures (Fig. 4E,F). This could be due to the presence of basic fibroblast growth factor in serum used in the culture medium (Yan and Wang, 2000a), or to *ngn1*’s reprogramming effect. In the chick retina, RA4$^+$ cells belong to the ganglion population. Vimentin$^+$ cells with thin, long processes, reminiscent of Muller glia or

progenitor cells, were also present, but only at places of large neural clusters (Fig. 4G,H). Overall, in *ngn1*-reprogrammed RPE cell culture, the number of cells expressing early photoreceptor markers far surpassed the number expressing early markers of other retinal cell types (Table 2), indicating that differentiating, photoreceptor-like cells were the major product of *ngn1*-induced reprogramming.

Because *ngn3* also induced the production of a large amount of visinin$^+$ cells from RPE cell culture (Fig. 2) and because *ngn3* in the retina promotes ganglion cell production (Ma et al., 2009), we analyzed RPE cell cultures infected RCAS-ngn3 to determine whether photoreceptor-like cells were the major product. RPE cell cultures infected with RCAS-ngn3 contained numerous clusters of neuron-like cells and often failed to reach confluency (Fig. 5A,B). These neuron-like cells began to die off 8 days after the administration of the virus. Immunostaining showed that 50-60% of the cells in the clusters are visinin$^+$ (Fig. 5C), and a significant portion (5-10%) were RA4$^+$ (Fig. 5D), indicating retinal ganglion-like cells constituted a significant portion of the reprogramming product.

Ultrastructural features resembling developing photoreceptors

The structural hallmarks of mature photoreceptors include an inner segment rich in mitochondria and an outer segment containing electron-dense membrane discs. However, when cultured as dissociated cells, developing photoreceptor cells rarely form the typical, elaborate outer segment with numerous discs stacked precisely (Saga et al. 1996). Instead, they develop ciliary expansions on the apex of the inner segment (Adler et al., 1984), and these ciliary expansions contain membranous, disc-like structures often irregularly arranged (Saga et al. 1996). Transmission electron microscopy showed that reprogrammed cells displayed cellular compartments densely populated with mitochondria (Fig. 6C,D), and closely resembling the inner segments of photoreceptor cells in E17 chick retina (Fig. 6G,H). These mitochondria-rich regions were not observed with control RPE cells, which contained characteristic pigment granules (Fig. 6A,B). On the apex of the inner segment, reprogrammed cells displayed ciliary expansions (Fig. 6C,D, black arrowhead), reminiscent of the developing outer segments of photoreceptors in E17 retina (Fig. 6G,H, black arrowhead) or in culture as described (Saga et al., 1996). The ciliary expansions contained membranous, disc-like structures (Fig. 6E,F, black arrowhead) that appeared similar to the developing outer segments of retinal photoreceptors in vivo (Fig. 6H,I).

Physiological traits of photoreceptors

One critical aspect to the prospect of the reprogrammed cells functioning as photoreceptors is whether they could develop the highly specialized physiological traits distinctive to photoreceptors. A well-known physiological trait of photoreceptors is light response. In the dark, photoreceptors are depolarized, and their intracellular Ca^{2+} levels are high. Upon exposure to light, photoreceptors become hyperpolarized, and their Ca^{2+} levels decrease as a result of continuing extrusion of calcium by the ion-exchangers after the light-driven closure of cGMP-gated channels (Yau and Nakatani, 1985). We used calcium imaging with fluo-4 AM and fluorescent photomicrography to monitor Ca^{2+} levels before and after light exposure. Due to their relatively low Ca^{2+} levels, RPE progeny cells in the control culture (infected with RCAS, Fig. 7A-C) and those lacking noticeable reprogramming in the experimental culture (Fig. 7D-J) were invisible. In contrast, reprogrammed cells (i.e., those displaying neural morphologies) were clearly visible with the fluorescent photomicrography. Upon a 10-second light exposure, the fluorescence intensities of reprogrammed cells decreased (Fig. 7D-F), indicating reductions in their Ca^{2+} levels. Reductions in fluorescent indentifies occurred in 20-40% of the cells. Computer-assisted calculation of integrated optical density (IOD) showed a reduction of ~30% in the fluorescent intensities after this brief light exposure (Fig. 7O). Prolonging the light exposure to 60 seconds produced a

further, but mild reduction in Ca^{2+} levels (Fig. 7G-J,P), thus ruling out the possibility that the Ca^{2+} level decrease was due to leakage over time. The dynamics of the Ca^{2+} level reductions are consistent with the reported high velocity activity of the Ca^{2+} extrusion mode of the exchanger during the initial 30 seconds (Schnetkamp, 1995).

As a reference, light responses by developing photoreceptor cells derived from E16 retina and cultured for 6 days (6 DIV) were similarly tested. The developing photoreceptor cells, identified by the presence of a lipid droplet (Fig. 7N, black arrowhead), responded to light by decreasing their Ca^{2+} levels in a manner that was similar to that of reprogrammed cells. Variations in the extent of Ca^{2+} reduction were observed with both reprogrammed and retinal cell populations (Fig. K-N,Q). This is expected, since these cells were not uniform in their levels of differentiation, and varied light responses have been reported among developing photoreceptors (Solessio et al., 2004).

To confirm the photoreceptor-like identity of reprogrammed cells showing light responses, post-Ca^{2+}-imaging immunostaining was carried out. Double-labeling showed that responding cells expressed red opsin and/or visinin (Fig. 8A-D,H). To address the question of whether the reduction in Ca^{2+} upon light exposure in reprogrammed cells was a light response, we carried out Ca^{2+} imaging in the presence of CNG channel blockers dichlorobenzamil and l-cis-diltiazem. We found no reductions in the Ca^{2+} levels of reprogrammed cells after exposure to light for 1 min in the presence of the blockers (Fig. 8E-G,I).

Visual recovery is another hallmark of photoreceptor physiology. In this process, light bleached photoreceptors, if provided with chromophore 11-cis-retinal or its analog 9-cis-retinal, recover their visual pigments. Visual recovery can be measured by an increase in Ca^{2+} level. To test whether the reprogrammed cells developed this trait, we monitored the Ca^{2+} levels of light-bleached, reprogrammed cells before and after the administration of 9-cis-retinal, and compared the response with that of developing photoreceptor cells in culture. To minimize the potential complication from RPE cells' ability to regenerate chromophore and to promote neural differentiation, cells from a primary culture infected with RCAS-ngn1 were reseeded at low density on polyornithine-treated coverslips. Once at lower density, the photoreceptor-like morphologies of the reprogrammed cells became more pronounced, with the lipid droplet-like feature clearly discernible (Fig. 9A,L, black arrowhead). We found that 2 minutes after the administration of 9-cis-retinal, Ca^{2+} levels in light-bleached, reprogrammed cells began to show noticeable increases (Fig. 9A-E,B1). This response occurred only in cells with advanced photoreceptor morphology, such as displaying a lipid droplet-like feature. Cells lacking conspicuous photoreceptor-like morphologies showed no response to 9-cis-retinal (Fig. 9A-E,B1, white arrowhead). Furthermore, response was more pronounced in cells with low Ca^{2+} levels after bleaching, presumably having responded strongly to the light during the bleaching as a result of advanced photoreceptor differentiation.

To verify that the increase was not due to vehicle (DMSO) or lapse of time, we subjected the same cells first to DMSO for 10 minutes and then to 9-cis-retinal for another 10 minutes. During the 10 minutes of treatment with only DMSO, Ca^{2+} levels remained essentially constant (Fig. 9F-K,C1). On the other hand, 2 minutes after the application of 9-cis-retinal, Ca^{2+} levels in cells displaying a lipid droplet-like feature showed detectable increases (Fig. 9L-Q,C1), while Ca^{2+} levels in cells lacking this conspicuous morphological feature remained unchanged (Fig. 9L-Q,C1, white arrowhead). The responses were similar in cultured developing photoreceptor cells derived from E19 chick retina (Fig. 9R-A1,D1).

Discussion

High efficiency of *ngn1*-induced reprogramming of RPE cells

The proliferative nature and plasticity of progeny cells make RPE a possible source of new photoreceptor cells. Key to this unconventional approach is to provide appropriate guidance to direct the progeny cells to the photoreceptor path. Among a number of genes and factors tested, a handful of bHLH proneural genes exhibited such a guiding activity. None of the homeodomain genes assayed was effective, despite of their important roles for the development of the retina and the photoreceptors. This, nonetheless, does not undermine their importance in retinal neurogenesis, because RPE progeny cells differ from retinal progenitors in many aspects. It is possible that either those competent bHLH proneural genes are better suited for the context of progeny cells, or the appropriate homedomain factor(s) remains to be identified.

Among the competent genes, *ngn1* (along with *ngn3*) ranked at the top by inducing the highest number of visinin$^+$ cells. When E15 RPE cells were used, *neuroD* became ineffective, indicating further its limited power in driving RPE progeny cells towards the photoreceptor pathway. *Ngn3* was similarly effective in inducing the production of visinin$^+$ cells. However, like with *ngn2*, reprogramming with *ngn3* resulted in significant amount of ganglion-like cells. Additionally, neuron-like cells in *ngn3*-reprogrammed culture died off, suggesting a detrimental effect of prolonged *ngn3* expression. Embryonic lethality has been observed with over- or mis-expression of *ngn3* (Ma et al., 2009). Overall, *ngn1* appears to be a better choice to reprogram RPE progeny cells to differentiate towards photoreceptors.

The order of potency of the bHLH genes seems consistent with their known or implicated roles in retinal neurogenesis. In the retina, *ngn2* is expressed throughout retinal neurogenesis in progenitor cells that may differentiate into all major types of retinal cells, including photoreceptors, rods and cones (Marquardt et al., 2001; Ma and Wang, 2006). *NeuroD* is predominantly expressed in postmitotic cells undergoing differentiation into photoreceptors, cones and rods (Yan and Wang, 1998; Yan and Wang, 2004; Liu et al., 2008). Expression of *ngn3* is switched off early, when retinal neurogenesis is still active and the expression *ath5*, *ngn2*, and *ash1* remains high (Ma et al., 2009). Temporally, expression of *ngn3* precedes the expression of *ngn1*. Spatially, expression of *ngn3*, but not *ngn1*, was also detected on the vitreal side, the prospective location of ganglion cells. Gain-of-function experiments showed a linear inductive relationship of *ngn3*→*ngn1* (Ma et al., 2009; Yan et al., submitted). Based on current information, *ngn1* seems best suited to be a major player in guiding a progenitor cell to the path of differentiating as a photoreceptor neuron. In the chick retina, *ngn1* expression coincides spatially and temporally with photoreceptor genesis and precedes *neuroD* expression (Yan et al., submitted). Overexpression of *ngn1* in retinal cells reduces the ganglion population, expands the photoreceptor population, and increases the number of cells expressing *neuroD*. SiRNA against *ngn1* reduces the photoreceptor population specifically (Yan et al., submitted). In Xenopus retina, the *ngn1*-related gene, *ngnr1*, specifically increases the photoreceptor population (Perron et al., 1999). In zebrafish retina, *ngn1* is expressed both in development and during photoreceptor regeneration after light-induced photoreceptor degeneration (Thummel et al., 2008).

Advanced photoreceptor differentiation

The induction of *visinin* expression in a large number of cells was concomitant with the generation of neural-like clusters in RPE cell cultures retrovirally transduced to express *ngn1*. The emergence of neural-like clusters from an otherwise non-neural cell culture suggests that *ngn1* not only induced a single gene, visinin, but also had initiated a reprogramming event. Reprogramming was further evidenced by the induction of several

transcription factors known to regulate photoreceptor differentiation, including *crx*, *neuroD*, *nr2e3*, *RaxL*, and *RXRγ*. The induction of these key regulators could have provided the molecular foundation for the reprogrammed cells to develop advanced photoreceptor traits, including the expression of phototransduction components, the formation of morphological characteristics, and acquiring hallmark physiological properties.

Photoreceptors develop unique structural and functional properties for their specific function in capturing photons and initiating the visual cascade. Structurally, photoreceptors contain inner segments that are rich in mitochondria and outer segments that consist of stacks of membranous discs. An inner segment-like structure packed with mitochondria was well formed in *ngn1*-reprogrammed cells. Some of the reprogrammed cells showed rudimentary outer segments, such as membranous expansion and electron-dense discs. Compared to inner segments, outer segment-like structures were observed at a much reduced frequency. This could be due to the non-permissive in vitro conditions for outer segment formation. It is known that even retinal photoreceptor cells rarely form outer segments in culture and can only develop irregularly arranged, membranous structures (Saga et al., 1996), as separating photoreceptors from the RPE prevents normal assembly of disk membranes (Kaplan et al., 1990). Under the conditions of our experiments, the reprogrammed cells were not expected to develop well-formed outer segments like those typically observed with mature photoreceptors immediately after isolation from an adult retina.

Physiologically, photoreceptors become hyperpolarized with decreased cytosolic Ca^{2+} upon light exposure. Another hallmark of photoreceptor physiology is visual recovery upon the administration of the chromophore to light-bleached photoreceptors. Both physiological hallmarks were displayed by reprogrammed cells generated from RPE cell cultures under the induction of *ngn1*. First, the reprogrammed cells reduced their Ca^{2+} levels upon light stimulation in a manner similar to cultured photoreceptor cells derived from developing chick retina. Second, administration of 9-cis-retinal to light-bleached, reprogrammed cells increased their Ca^{2+} levels. The increases were comparable to those observed with light-bleached, cultured developing photoreceptor cells derived from the retina. The physiological resemblances indicate advanced photoreceptor differentiation of the reprogrammed cells.

Reprogramming RPE with *ngn1* as an effective approach to produce photoreceptor-like cells

Because of the great potential of photoreceptor-replacement in saving sight, much attention has been directed at identifying source of new, differentiating photoreceptor cells. Retinal stem cells would be one of the ideal sources of new photoreceptor cells. However, their presence in the mammalian retina remains controversial. Early reports indicated that the ciliary epithelium (CE) in the mammalian eye contains retinal stem cells (Tropepe et al., 2000; Ahmad et al., 2000), but a recent study shows that CE-derived spheres consist of proliferating pigmented CE cells rather than retinal stem cells (Cicero et al., 2009). Muller glial cells in various species, including mammals, have recently been shown to posses certain retinal progenitor cell properties, but their capabilities to efficiently give rise to photoreceptors remain to be demonstrated (for a review, see Ohta et al., 2008). Outside the neural retina, various cells/tissues of the mammalian eye are also investigated, including the iris pigment epithelium, the ciliary body, and limbal epithelium. These cells/tissues of the eye give minute amounts, if any, of photoreceptor-like cells (Ohta et al., 2008). The low yield reflects may reflect the biological nature of those specific tissues, or the experimental approaches used, as none of the studies have used *ngn1* to initiate photoreceptor differentiation program in those non-neural cells/tissues of the eye. Mammalian stem cells of various origins (brain, bone marrow, and embryos) have been intensively explored (Takahashi et al., 1998; Kicic et al., 2003; Chen et al., 2006; Meyer et al., 2006; Banin et al., 2006; Lamba et al., 2006; Osakada et al., 2008; Lamba et al., 2009). Significant progress has

been reported in guiding embryonic stem cells to differentiate into photoreceptors (Osakada et al., 2008; Lamba et al., 2009). Nonetheless, challenges remain, such as the efficiency at which photoreceptors are produced (Reh, 2006; MacLaren and Pearson, 2007; Klassen and Reubinoff, 2008) and the mode of action of the donor (stem) cells (Gaillard and Sauve, 2007).

We have tested a different approach of producing differentiating, photoreceptor-like cells, and our data show that *ngn1* induced as high as 80% of the cells present in areas of an RPE cell culture to begin differentiation towards photoreceptor cells. The reprogrammed cells expressed transcription factors regulating photoreceptor differentiation and functional components of the phototransduction pathway. They displayed similarities with developing photoreceptor cells in ultrastructure, subcellular localization of red opsin, and in physiological responses to light and to 9-cis-retinal. The advanced photoreceptor differentiation and the high efficiency support RPE reprogramming by *ngn1* as an attractive approach to generate new, differentiating photoreceptor cells.

Acknowledgments

We thank Dr. Steven Hughes for the retroviral cloning vectors, Dr. Steven McLoon for RA4 mAb, Drs. Marie Burns and Krzysztof Palczewski for suggestions on experiments involving 9-cis-retinal, and Dr. Christine Curcio for guidance on electron photomicrography. This study is supported by NIH/NEI EY011640, EyeSight Foundation research grant FY2008-09-134, and an unrestricted grant to the UAB Department of Ophthalmology from Research to Prevent Blindness. XL is a recipient of the International Retinal Research Foundation Postdoctoral Scholar Award.

Grant support: NIH/NEI grant EY11640, EyeSight Foundation research grant FY2008-09-134, the China Scholarship Council, and an unrestricted grant to the UAB Department of Ophthalmology from Research to Prevent Blindness.

References

Adler R, Curcio C, Hicks D, Price D, Wong F. Cell death in age-related macular degeneration. Mol Vis 1999;5:31. [PubMed: 10562655]

Adler R, Lindsey JD, Elsner CL. Expression of cone-like properties by chick embryo neural retina cells in glial-free monolayer cultures. J Cell Biol 1984;99:1173–1178. [PubMed: 6470040]

Ahmad I, Tang L, Pham H. Identification of neural progenitors in the adult mammalian eye. Biochem Biophys Res Commun 2000;270:517–521. [PubMed: 10753656]

Aramant RB, Seiler MJ. Retinal transplantation--advantages of intact fetal sheets. Prog Retin Eye Res 2002;21:57–73. [PubMed: 11906811]

Austin CP, Feldman DE, Ida JA, Cepko CL. Vertebrate retinal ganglion cells are selected from competent progenitors by the action of Notch. Development 1995;121:3637–3650. [PubMed: 8582277]

Banin E, Obolensky A, Idelson M, Hemo I, Reinhardtz E, Pikarsky E, Ben-Hur T, Reubinoff B. Retinal incorporation and differentiation of neural precursors derived from human embryonic stem cells. Stem Cells 2006;24:246–257. [PubMed: 16123388]

Belecky-Adams T, Tomarev S, Li H-S, Ploder L, McInnes RR, Sundin O, Adler R. Pax-6, Prox1, and Chx10 homeobox gene expression correlates with phenotyppic fate of retinal precursor cells. Invest Ophthalmol Vis Sci 38:1293–303. 1007. [PubMed: 9191592]

Bennett J. Gene therapy for Leber congenital amaurosis. Novartis Found Symp 2004;255:195–202. [PubMed: 14750605]

Bennett J. Retinal progenitor cells--timing is everything. N Engl J Med 2007;356:1577–1579. [PubMed: 17429090]

Bisgrove DA, Godbout R. Differential expression of AP-2alpha and AP-2beta in the developing chick retina: repression of R-FABP promoter activity by AP-2. Dev Dyn 1999;214:195–206. [PubMed: 10090146]

Bok D. The retinal pigment epithelium: a versatile partner in vision. J Cell Sci Suppl 1993;17:189–195. [PubMed: 8144697]

Brown NL, Patel S, Brzezinski J, Glaser T. Math5 is required for retinal ganglion cell and optic nerve formation. Development 2001;128:2497–2508. [PubMed: 11493566]

Burmeister M, Novak J, Liang MY, Basu S, Ploder L, Hawes NL, Vidgen D, Hoover F, Goldman D, Kalnins VI, Roderick TH, Taylor BA, Hankin MH, McInnes RR. Ocular retardation mouse caused by Chx10 homeobox null allele: impaired retinal progenitor proliferation and bipolar cell differentiation. Nat Genet 1996;12:376–384. [PubMed: 8630490]

Chen CM, Cepko CL. The chicken RaxL gene plays a role in the initiation of photoreceptor differentiation. Development 2002;129:5363–5375. [PubMed: 12403708]

Chen S, Wang Q-L, Nie Z, Sun H, Lennon G, Copeland NG, Gilbert DJ, Kenkins NA, Zack D. Crx, a novel otx-like paired-homeodomain protein, binds to and transactivates photoreceptor cell-specific genes. Neuron 1997;19:1017–1030. [PubMed: 9390516]

Chen Y, Teng FY, Tang BL. Coaxing bone marrow stromal mesenchymal stem cells towards neuronal differentiation: progress and uncertainties. Cell Mol Life Sci 2006;63:1649–1657. [PubMed: 16786223]

Cicero SA, Johnson D, Reyntjens S, Frase S, Connell S, Chow LM, Baker SJ, Sorrentino BP, Dyer MA. Cells previously identified as retinal stem cells are pigmented ciliary epithelial cells. Proc Natl Acad Sci U S A 2009;106:6685–6690. [PubMed: 19346468]

Ellis JH, Richards DE, Rogers JH. Calretinin and calbindin in the retina of the developing chick. Cell Tissue Res 1991;264:197–208. [PubMed: 1878940]

Fekete DM, Cepko CL. Replication-competent retroviral vectors encoding alkaline phosphatase reveal spatial restriction of viral gene expression/transduction in the chick embryo. Mol Cell Biol 1993;13:2604–2613. [PubMed: 8455633]

Fischer AJ, Stanke JJ, Aloisio G, Hoy H, Stell WK. Heterogeneity of horizontal cells in the chicken retina. J Comp Neurol 2007;500:1154–1171. [PubMed: 17183536]

Furukawa Y, Morrow EM, Cepko CL. Crx, a novel otx-like homeobox gene, shows photoreceptor-specific expression and regulates photoreceptor differentiation. Cell 1997;91:531–541. [PubMed: 9390562]

Gaillard F, Sauvé Y. Cell-based therapy for retina degeneration: the promise of a cure. Vision Res 2007;47:2815–2824. [PubMed: 17719072]

Hatakenaka S, Kiyama H, Tohyama M, Miki N. Immunohistochemical localization of chick retinal 24 kdalton protein (visinin) in various vertebrate retinae. Brain Res 1985;331:209–215. [PubMed: 3886079]

Herman J-P, Victor JC, Sanes JR. Developmentally regulated and spatially restricted antigens of radial glial cells. Dev Dyn 1993;197:307–318. [PubMed: 8292827]

Hughes SH, Greenhouse JJ, Petropoulos CJ, Sutrave P. Adaptor plasmids simplify the insertion of foreign DNA into helper-independent retroviral vectors. J Virol 1987;61:4–12.

Hunt RC, Davis AA. Altered expression of keratin and vimentin in human retinal pigment epithelial cells in vivo and in vitro. J Cell Physiol 1990;145:187–199. [PubMed: 1700982]

Kaplan MW, Iwata RT, Sterrett CB. Retinal detachment prevents normal assembly of disk membranes in vitro. Invest Ophthalmol Vis Sci 1990;31:1–8. [PubMed: 2298531]

Kicic A, Shen WY, Wilson AS, Constable IJ, Robertson T, Rakoczy PE. Differentiation of marrow stromal cells into photoreceptors in the rat eye. J Neurosci 2003;23:7742–7749. [PubMed: 12944502]

Klassen H, Reubinoff B. Stem cells in a new light. Nat Biotechnol 2008;26:187–88. [PubMed: 18259172]

Lamba DA, Karl MO, Ware CB, Reh TA. Efficient generation of retinal progenitor cells from human embryonic stem cells. Proc Natl Acad Sci USA 2006;103:12769–12774. [PubMed: 16908856]

Lamba DA, Gust J, Reh TA. Transplantation of human embryonic stem cell-derived photoreceptors restores some visual function in Crx-deficient mice. Cell Stem Cell 2009;9:73–79. [PubMed: 19128794]

Lavail MM. Legacy of the RCS rat: impact of a seminal study on retinal cell biology and retinal degenerative diseases. Prog Brain Res 2001;131:617–627. [PubMed: 11420975]

Li C-M, Yan R-T, Wang S-Z. Misexpression of cNSCL1 disrupts retinal development. Mol Cell Neurosci 1999;14:17–27. [PubMed: 10433814]

Li C-M, Yan R-T, Wang S-Z. Misexpression of chick NSCL2 causes atrophy of Müller glia and photoreceptor cells. Invest Ophthalmol Vis Sci 2001;42:3103–3109. [PubMed: 11726609]

Li X, Ma W, Zhuo Y, Yan R-T, Wang S-Z. Using neurogenin to reprogram chick RPE to produce photoreceptor-like neurons. Invest Ophthalmol Vis Sci. 2009 In press.

Liang L, Ma W, Yan R-T, Zhang H, Wang S-Z. Exploring RPE as a source of photoreceptors: differentiation and integration of transdifferentiating cells grafted into embryonic chick eyes. Invest. Ophthalmol Vis Sci 2006;47:5066–5074. [PubMed: 17065528]

Liang L, Yan R-T, Li X, Chimento M, Wang S-Z. Reprogramming progeny cells of embryonic RPE to produce photoreceptors: development of advanced photoreceptor traits under the induction of *neuroD*. Invest Ophthalmol Vis Sci 2008;49:4145–4153. [PubMed: 18469196]

Liu H, Etter P, Hayes S, Jones I, Nelson B, Hartman B, Forrest D, Reh T. NeuroD1 regulates expression of thyroid hormone receptor β2 and cone opsins in the developing mouse retina. J Neurosci 2008;28:749–756. [PubMed: 18199774]

Liu W, Wang JH, Xiang M. Specific expression of the LIM/homeodomain protein Lim-1 in horizontal cells during retinogenesis. Dev Dyn 2000;217:320–25. [PubMed: 10741426]

Ma W, Wang S-Z. The final fates of neurogenin2-expressing cells include all major neuron types in the mouse retina. Mol Cell Neurosci 2006;31:463–469. [PubMed: 16364654]

Ma W, Yan R-T, Li X, Wang S-Z. Reprogramming RPE cell differentiation in vivo and in vitro with Sox2. Stem Cells. 2009 In press.

Ma W, Yan R-T, Mao W, Wang S-Z. Neurogenin3 promotes early retinal neurogenesis. Mol Cell Neurosci 2009;40:187–198. [PubMed: 19028584]

Ma W, Yan R-T, Xie W, Wang S-Z. bHLH genes *cath5* and *cNSCL1* promote bFGF-stimulated RPE cells to transdifferentiate towards retinal ganglion cells. Dev Biol 2004;265:320–328. [PubMed: 14732395]

MacLaren RE, Pearson RA. Stem cell therapy and the retina. Eye 2007;21:1352–1359. [PubMed: 17914439]

MacLaren RE, Pearson RA, MacNeil A, Douglas RH, Salt TE, Akimoto M, Swaroop A, Sowden JC, Ali RR. Retinal repair by transplantation of photoreceptor precursors. Nature 2006;444:203–207. [PubMed: 17093405]

MacNeil MA, Gaul PA. Biocytin wide-field bipolar cells in rabbit retina selectively contact blue cones. J Comp Neurol 2008;506:6–15. [PubMed: 17990268]

Mao W, Yan R-T, Wang S-Z. Proneural gene ash1 promotes amacrine cell production in the chick retina. Dev Neurobiol 2009;69:88–104. [PubMed: 19067322]

Mao W, Yan R-T, Wang S-Z. Reprogramming chick RPE progeny cells to differentiate towards retinal neurons by *ash1*. Mol Vis 2008;14:2309–2320. [PubMed: 19093008]

Marquardt T, Ashery-Padan R, Andrejewski N, Scardigli R, Guillemot F, Gruss P. Pax6 is required for the multipotent state of retinal progenitor cells. Cell 2001;105:43–55. [PubMed: 11301001]

Mathers PH, Jamrich M. Regulation of eye formation by the Rx and pax6 homeobox genes. Cel. Mol Life Sci 2000;57:186–194.

McLoon SC, Barnes RB. Early differentiation of retinal ganglion cells: an axonal protein expressed by premigratory and migrating retinal ganglion cells. J Neurosci 1989;9:1424–1432. [PubMed: 2703885]

Mears AJ, Kondo M, Swain PK, Takada Y, Bush RA, Saunders TL, Sieving PA, Swaroop A. Nrl is required for rod photoreceptor development. Nat Genet 2001;29:447–452. [PubMed: 11694879]

Meyer JS, Katz ML, Maruniak JA, Kirk MD. Embryonic stem cell-derived neural progenitors incorporate into degenerating retina and enhance survival of host photoreceptors. Stem Cells 2006;24:274–283. [PubMed: 16123383]

Milam AH, Rose L, Cideciyan AV, Barakat MR, Tang WX, Gupta N, Aleman TS, Wright AF, Stone EM, Sheffield VC, Jacobson SG. The nuclear receptor NR2E3 plays a role in human retinal photoreceptor differentiation and degeneration. Proc Natl Acad Sci USA 2002;99:473–478. [PubMed: 11773633]

Ohta K, Ito A, Tanaka H. Neural stem/progenitor cells in the vertebrate eye. Develop Growth Differ 2008;50:253–259.

Osakada F, Ikeda H, Mandai M, Wataya T, Watanabe K, Yoshimura N, Akaike A, Sasai Y, Takahashi M. Toward the generation of rod and cone photoreceptors from mouse, monkey and human embryonic stem cells. Nat Biotechnol 2008;26:215–224. [PubMed: 18246062]

Otteson DC, Hitchcock PF. Stem cells in the teleost retina: persistent neurogenesis and injury-induced regeneration. Vision Res 2003;43:927–936. [PubMed: 12668062]

Park CM, Hollenberg MJ. Basic fibroblast growth factor induces retinal regeneration in vivo. Dev Biol 134:201–205. [PubMed: 2731647]

Pennesi ME, Cho JH, Yang Z, Wu SH, Zhang J, Wu SM, Tsai MJ. BETA2/NeuroD1 null mice: a new model for transcription factor-dependent photoreceptor degeneration. J Neurosci 2003;23:453–461. [PubMed: 12533605]

Perron M, Opdecamp K, Butler K, Harris WA, Bellefroid EJ. X-ngnr-1 and Xath3 promote ectopic expression of sensory neuron markers in the neurula ectoderm and have distinct inducing properties in the retina. Proc Natl Acad Sci USA 1999;96:14996–15001. [PubMed: 10611326]

Pittack C, Jones M, Reh TA. Basic fibroblast growth factor induces retinal pigment epithelium to generate neural retina in vitro. Development 1991;113:577–588. [PubMed: 1782868]

Raymond PA. Retinal regeneration in teleost fish. Ciba Found Symp 1991;160:171–186. [PubMed: 1752162]

Reddy ST, Stoker AW, Bissell MJ. Expression of Rous sarcoma virus-derived retroviral vectors in the avian blastoderm: potential as stable genetic markers. Proc Natl Acad Sci U S A 1991;88:10505–10509. [PubMed: 1660139]

Reh TA. Neurobiology: right timing for retina repair. Nature 2006;444:156–157. [PubMed: 17093406]

Rizzolo LJ, Chen X, Weitzman M, Sun R, Zhang H. Analysis of the RPE transcriptome reveals dynamic changes during the development of the outer blood-retinal barrier. Mol Vis 2007;13:1259–1273. [PubMed: 17679949]

Roberts MR, Hendrickson A, McGuire CR, Reh TA. Retinoid X receptor (gamma) is necessary to establish the S-opsin gradient in cone photoreceptors of the developing mouse retina. Invest Ophthalmol Vis Sci 2005;46:2897–2904. [PubMed: 16043864]

Saga T, Scheurer D, Adler R. Development and maintenance of outer segments by isolated chick embryo photoreceptor cells in culture. Invest Ophthalmol Vis Sci 1996;37:561–573. [PubMed: 8595956]

Sakami S, Etter P, Reh TA. Activin signaling limits the competence for retinal regeneration from the pigmented epithelium. Mech Dev 2008;125:106–116. [PubMed: 18042353]

Schnetkamp PP. How does the retinal rod Na-Ca+K exchanger regulate cytosolic free Ca^{2+}? J Biol Chem 1995;270:13231–13239. [PubMed: 7539424]

Solessio E, Mani SS, Cuenca N, Engbretson GA, Barlow RB, Knox BE. Developmental regulation of calcium-dependent feedback in Xenopus rods. J Gen Physiol 2004;124:569–585. [PubMed: 15504902]

Stenkamp DL, Cameron DA. Cellular pattern formation in the retina: retinal regeneration as a model system. Mol Vis 2002;8:280–293. [PubMed: 12181523]

Takahashi M, Palmer TD, Takahashi J, Gage FH. Widespread integration and survival of adult-derived neural progenitor cells in the developing optic retina. Mol Cell Neurosci 1998;12:340–348. [PubMed: 9888988]

Taranova OV, Magness ST, Fagan BM, Wu Y, Surzenko N, Hutton SR, Pevny LH. SOX2 is a dose-dependent regulator of retinal neural progenitor competence. Genes & Dev 2006;20:1187–1202. [PubMed: 16651659]

Thummel R, Kassen SC, Enright JM, Nelson CM, Montgomery JE, Hyde DR. Characterization of Müller glia and neuronal progenitors during adult zebrafish retinal regeneration. Exp Eye Res 2008;87:433–444. [PubMed: 18718467]

Tomita K, Moriyoshi K, Nakanishi S, Guillemot F, Kageyama R. Mammalian achaete-scute and atonal homologs regulate neuronal versus glial fate determination in the central nervous system. EMBO J 2000;19:5460–5472. [PubMed: 11032813]

Tomita K, Nakanishi S, Guillemot F, Kageyama R. Mash1 promotes neuronal differentiation in the retina. Genes Cells 1996;1:765–774. [PubMed: 9077445]

Toy J, Yang JM, Leppert GS, Sundin OH. The optx2 homeobox gene is expressed in early precursors of the eye and activates retina-specific genes. Proc Natl Acad Sci U S A 1998;95(18):10643–10648. [PubMed: 9724757]

Tropepe V, Coles BLK, Chaisson BJ, Horsford DJ, Elia AJ, McGinnis RR, van der Kooy D. Retinal stem cells in the adult mouse eye. Science 2000;287:2032–2036. [PubMed: 10720333]

Waid DK, McLoon SC. Immediate differentiation of ganglion cells following mitosis in the developing retina. Neuron 1995;14:117–124. [PubMed: 7826629]

Wang SW, Kim BS, Ding K, Wang H, Sun D, Johnson RL, Klein WH, Gan L. Requirement for math5 in the development of RGCs. Genes Dev 2001;15:24–29. [PubMed: 11156601]

Xiang M, Zhou L, Macke JP, Yoshioka T, Hendry SH, Eddy RL, Shows TB, Nathans J. The Brn-3 family of POU-domain factors: primary structure, binding specificity, and expression in subsets of retinal ganglion cells and somatosensory neurons. J Neurosci 1995;15:4762–4785. [PubMed: 7623109]

Xie W, Yan R-T, Ma W, Wang S-Z. Enhanced retinal ganglion cell differentiation by *ath5* and *NSCL1* coexpression. Invest Ophthalmol Vis Sci 2004;45:2922–2928. [PubMed: 15326103]

Yamagata K, Goto K, Kuo CH, Kondo H, Miki N. Visinin: a novel calcium binding protein expressed in retinal cone cells. Neuron 1990;4:469–476. [PubMed: 2317380]

Yan R-T, He L, Wang S-Z. Pro-photoreceptor activity of chick *neurogenin1*. Invest Ophthalmol Vis Sci. 2009 in press.

Yan R-T, Ma W, Wang S-Z. neurogenin2 elicits the genesis of retinal neurons from cultures of non-neural cells. Proc Natl Acad Sci USA 2001;98:15014–15019. [PubMed: 11752450]

Yan R-T, Wang S-Z. neuroD induces photoreceptor cell overproduction in vivo and de novo generation in vitro. J Neurobiol 1998;36:485–496. [PubMed: 9740021]

Yan R-T, Wang S-Z. Differential induction of gene expression by basic fibroblast growth factor and *neuroD* in cultured retinal pigment epithelial cells. Visual Neurosci 2000a;17:157–164.

Yan R-T, Wang S-Z. Expression of an array of photoreceptor genes in chick embryonic RPE cell cultures under the induction of neuroD. Neurosci Letters 2000b;280:83–86.

Yan R-T, Wang S-Z. Requirement of NeuroD for photoreceptor formation in the chick retina. Invest Ophthalmol Vis Sci 2004;45:48–58. [PubMed: 14691153]

Yau KW, Nakatani K. Light-induced reduction of cytoplasmic free calcium in retinal rod outer segment. Nature 1985;313:579–582. [PubMed: 2578628]

Young MJ. Stem cells in the mammalian eye: a tool for retinal repair. APMIS 2005;113:845–857. [PubMed: 16480454]

Zhao S, Thornquist SC, Barnstable CJ. In vitro transdifferentiation of embryonic rat pigment epithelium to neural retina. Brain Res 1995;677:300–310. [PubMed: 7552256]

Zhu CC, Dyer MA, Uchikawa M, Kondoh H, Lagutin OV, Oliver G. Six3-mediated auto repression and eye development requires its interaction with members of the Groucho-related family of co-repressors. Development 2002;129:2835–49. [PubMed: 12050133]

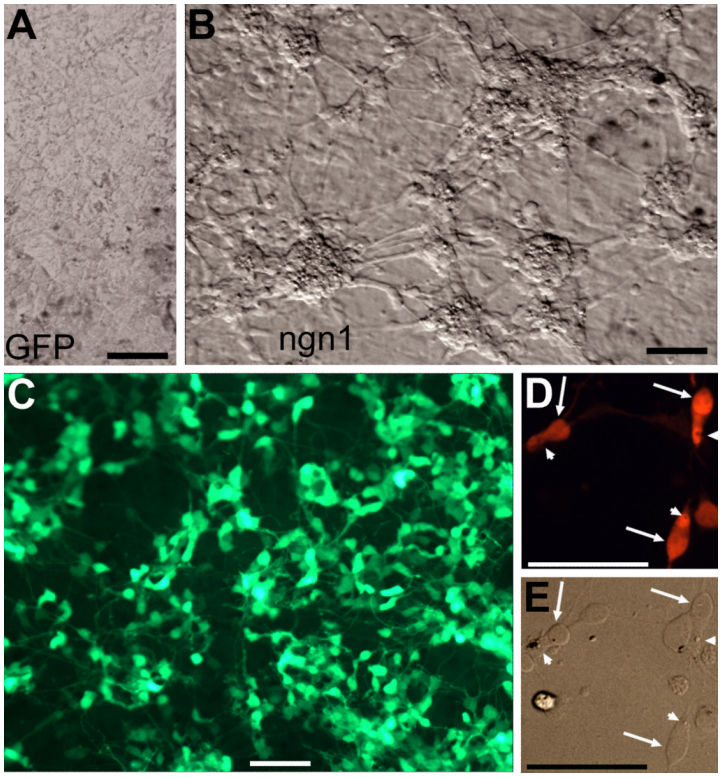

Fig. 1.

RPE cell cultures reprogrammed by *ngn1*. A,B: Bright-field views of a control culture infected with retrovirus RCAS-GFP (A) and a reprogrammed culture infected with RCAS-ngn1 (B). Red asterisks (*) in B mark cells clusters, which are absent in the control. C: Epi-fluorescence of visinin immunostaining of a *ngn1*-reprogrammed culture. D,E: Morphology of visinin^{+} cells viewed with bright-field (E) and epi-fluorescence (D). Arrows point to the cell body, and arrowheads point to a structural feature reminiscent of the lipid-droplet typically present in chick photoreceptors. Scale bars: 50 μm. A magenta-green copy is available as supplementary data.

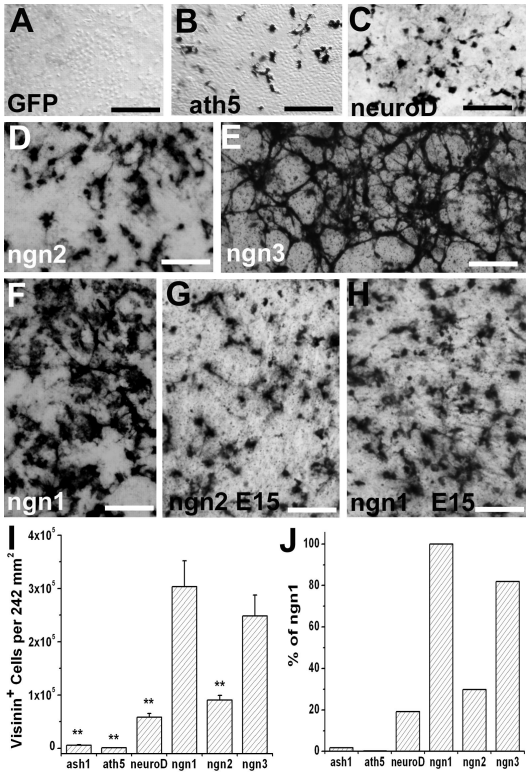

Fig. 2.

Prevalence of visinin$^+$ cells in RPE cell cultures subjected to reprogramming by various factors/genes. A-F: Representative images of immunodetection of visinin in E6 RPE cell cultures infected with retrovirus RCAS expressing GFP (A; a negative control), *ath5* (B), *neuroD* (C), *ngn2* (D), *ngn3* (E), and *ngn1* (F). G,H: Immunostaining for visinin in an E15 RPE cell culture infected with RCAS-ngn2 (G) or RCAS-ngn1 (H). I: Calculated numbers of visinin$^+$ cells per 242 mm^2 area in E6 RPE cell cultures reprogrammed with the different genes as shown. J: Calculated percentage of visinin$^+$ cells in E6 RPE cell cultures reprogrammed with the different genes as shown against *ngn1*-reprogrmaed culture. Scale bars: 100 μm.

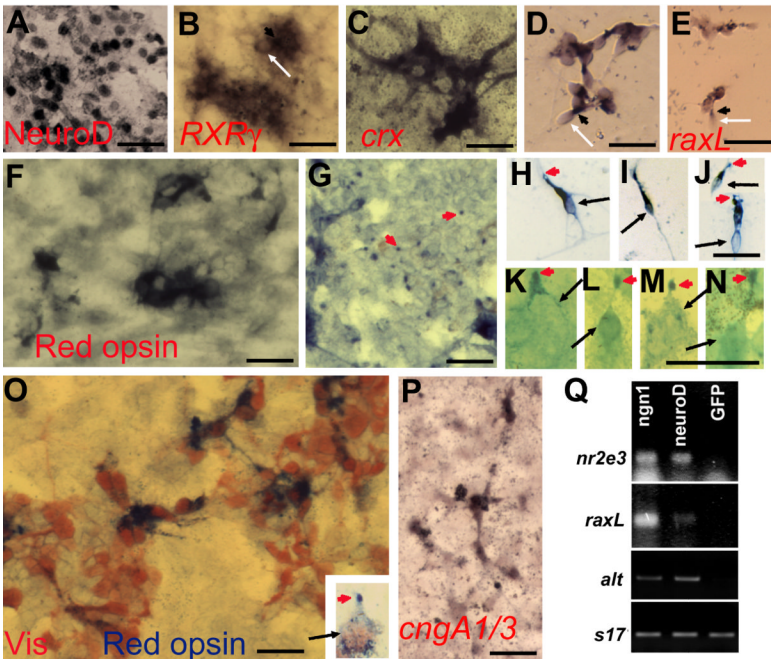

Fig. 3.

Expression of photoreceptor-specific genes in RPE cell cultures infected with RCAS-ngn1. A-E: Induction of transcription factors important for photoreceptor differentiation in *ngn1*-reprogrammed cultures. A: Immunostaining for NeuroD. B: In situ hybridization for *RXRγ* mRNA. C,D: In situ hybridization for *crx* mRNA in primary culture (C) and in re-seeded culture (D). E: In situ hybridization for *raxL* mRNA. F-K: Expression of phototransduction components in *ngn1*-reprogrammed cultures. F,G: Anti-red opsin immunostaining of the cell body (F) and dot-like structures at places (of the culture) where more pigmented RPE cells were present (G). H-N: Morphologies of red opsin^{+} cells in a re-seeded culture under a 40x objective (H-J) or in a primary culture under a 100x objective (K-N). Arrows point to cell bodies. Arrowheads point to cells' apices decorated by anti-red opsin immunostaining. O: Double-staining with antibodies against visinin (in red) and red opsin (in blue). Inset: A higher magnification view of a double-labeled cell showing its cell body (arrow) and its apex decorated by anti-red opsin (arrowhead). P: In situ hybridization detection of the α-subunits of cone and rod CNG channels (*cngA1/3*). Q: RT-PCR detection of the expression of two transcription factors (*nr2e3* and *raxL*), one phototransduction component (α-transducin, *alt*), and a control gene (*s17*) in cultures expressing RCAS-*ngn1*, RCAS-*neuroD*, or RCAS-GFP. Scale bars: 25 μm. A magenta-green copy is available as supplementary data.

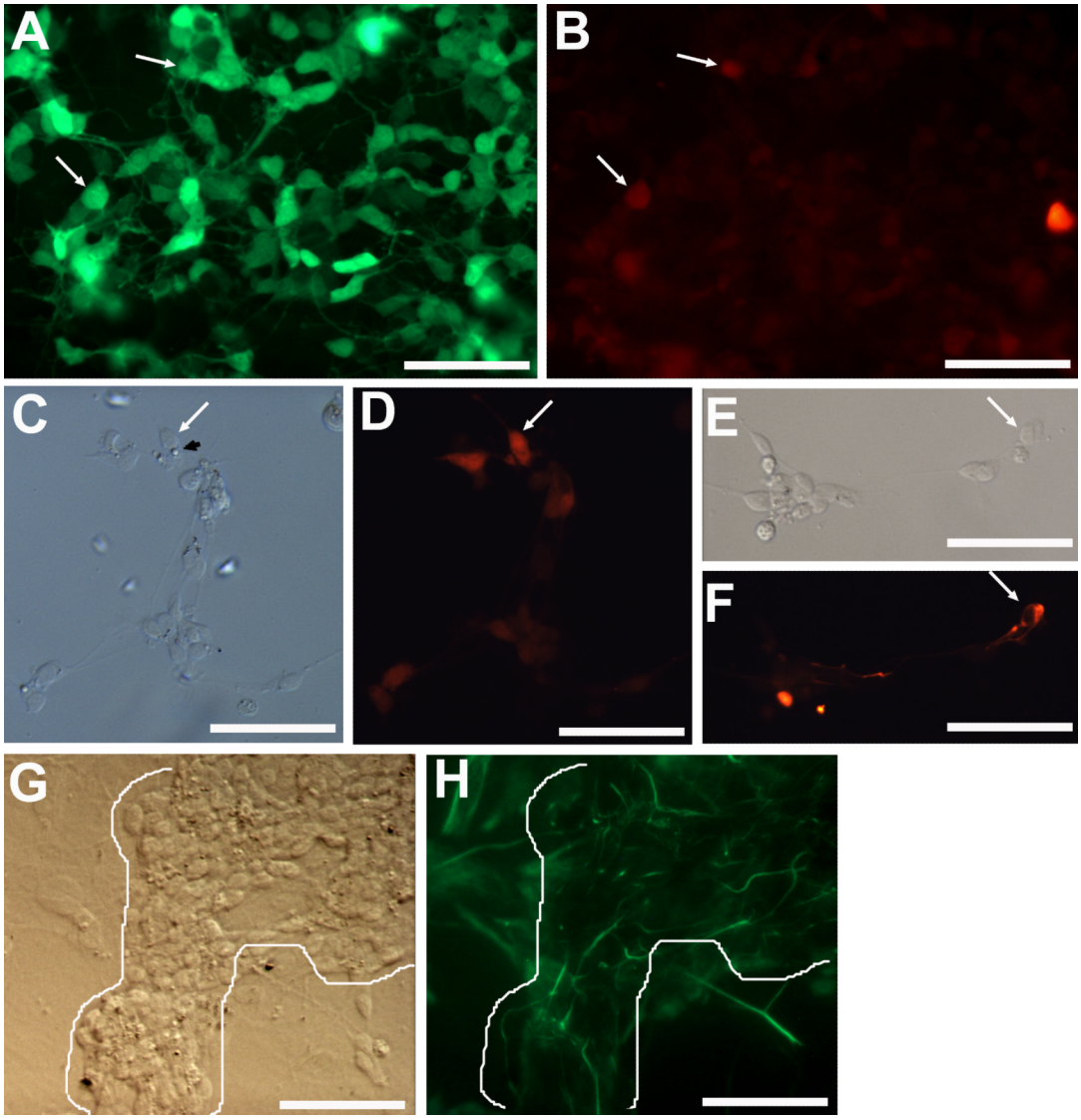

Fig. 4.

Detection of markers of various retinal cell types in *ngn1*-reprogrammed cultures. A,B: Double-labeling for visinin (A) and calretinin (B) in a primary, reprogrammed culture. Arrows point to double-labeled cells. C,D: Morphologies of calretinin$^+$ cells in a reseeded culture, viewed with bright field (C) or epi-fluorescence (D). The arrow points to a calretinin$^+$ cell displaying a lipid-droplet-like structure. E,F: An RA4$^+$ cell (arrow) with a long process in a reseeded culture viewed with bright field (E) or epi-fluorescence (F). G,H: Vimentin$^+$ cells in a primary, reprogrammed culture viewed with bright field (G) or epi-fluorescence (H). Note: Long processes that were immuno-positive were present only at places occupied by cell clusters (outlined). Scale bars: 50 μm. A magenta-green copy is available as supplementary data.

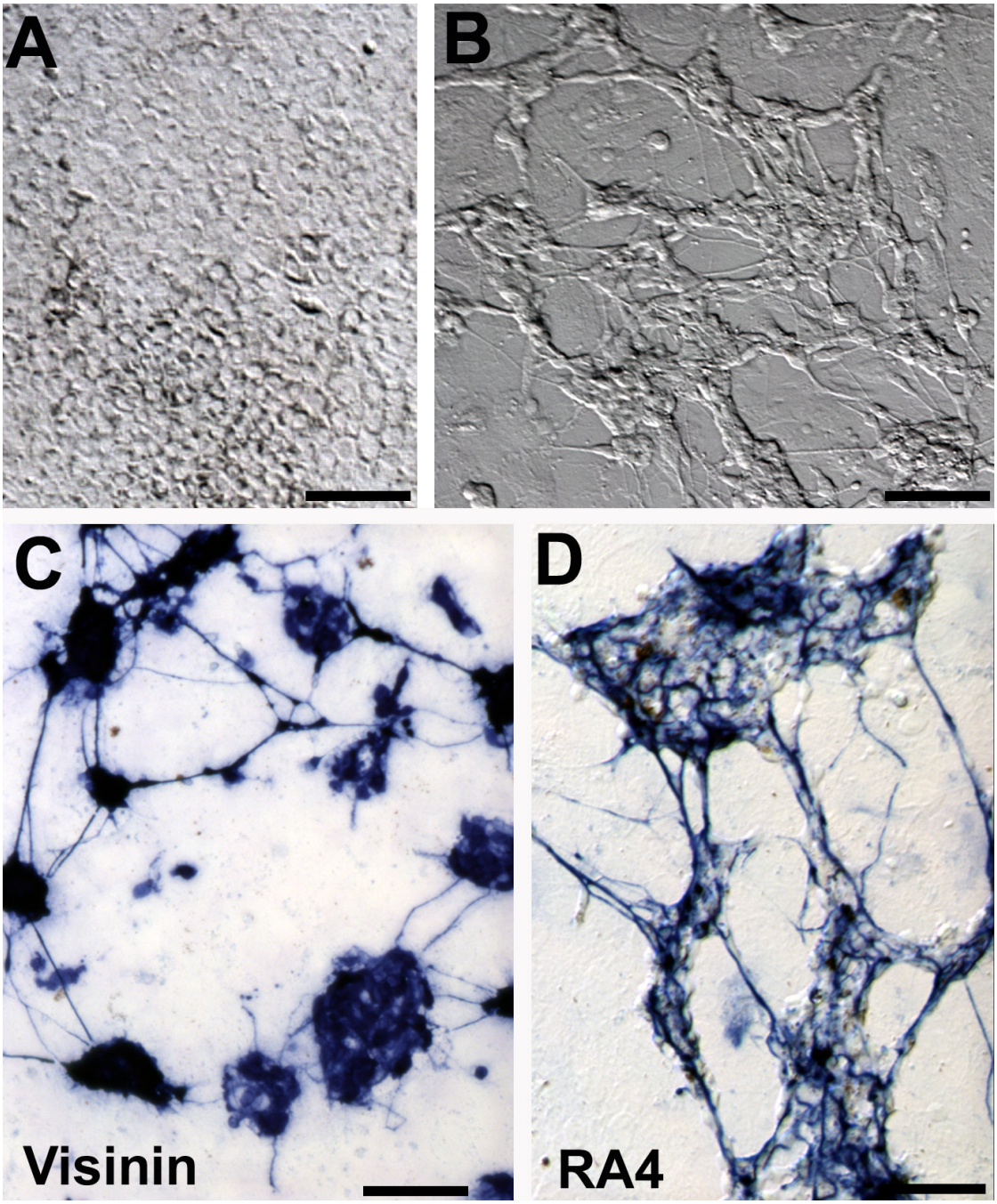

Fig. 5.

Ngn3-reprogrammed E6 RPE cell cultures. A,B: Bright-field views of a control culture infected with RCAS-GFP (A) and a culture infected by RCAS-ngn3 (B). C,D: Anti-visinin (C) and RA4 (D) immunostaining of cultures infected with RCAS-ngn3. Scale bars: 50 μm.

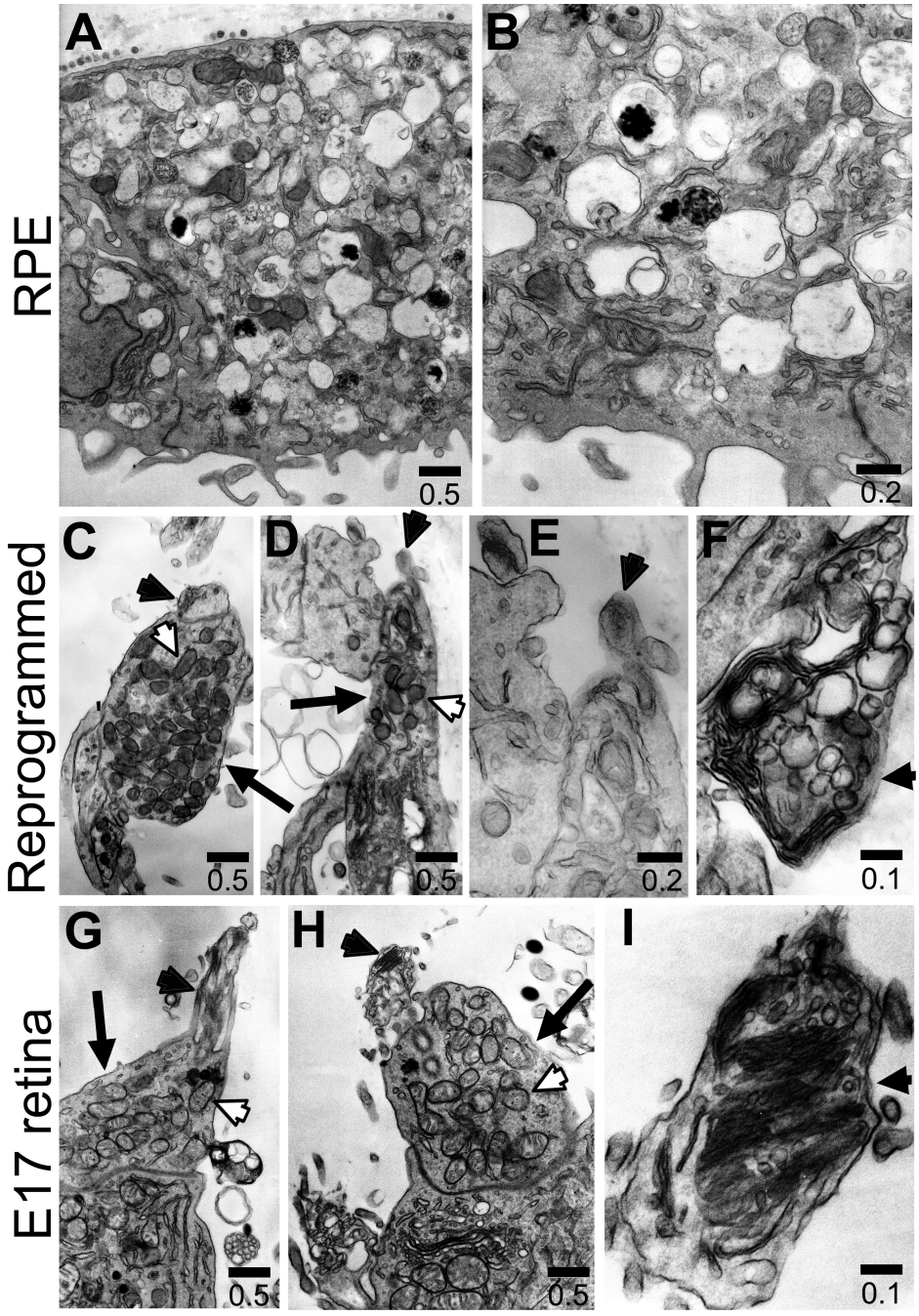

Fig. 6.

Ultrastructures examined with electron micrography. A-B: Cells in a control RPE cell culture. C-F: *ngn1*-reprogrammed cells. D-I: Developing photoreceptors in E17 chick retina. Arrows: Inner segment; arrowheads: membranous expansion atop inner segments; white arrowheads: mitochondria. The scale bars are in μm.

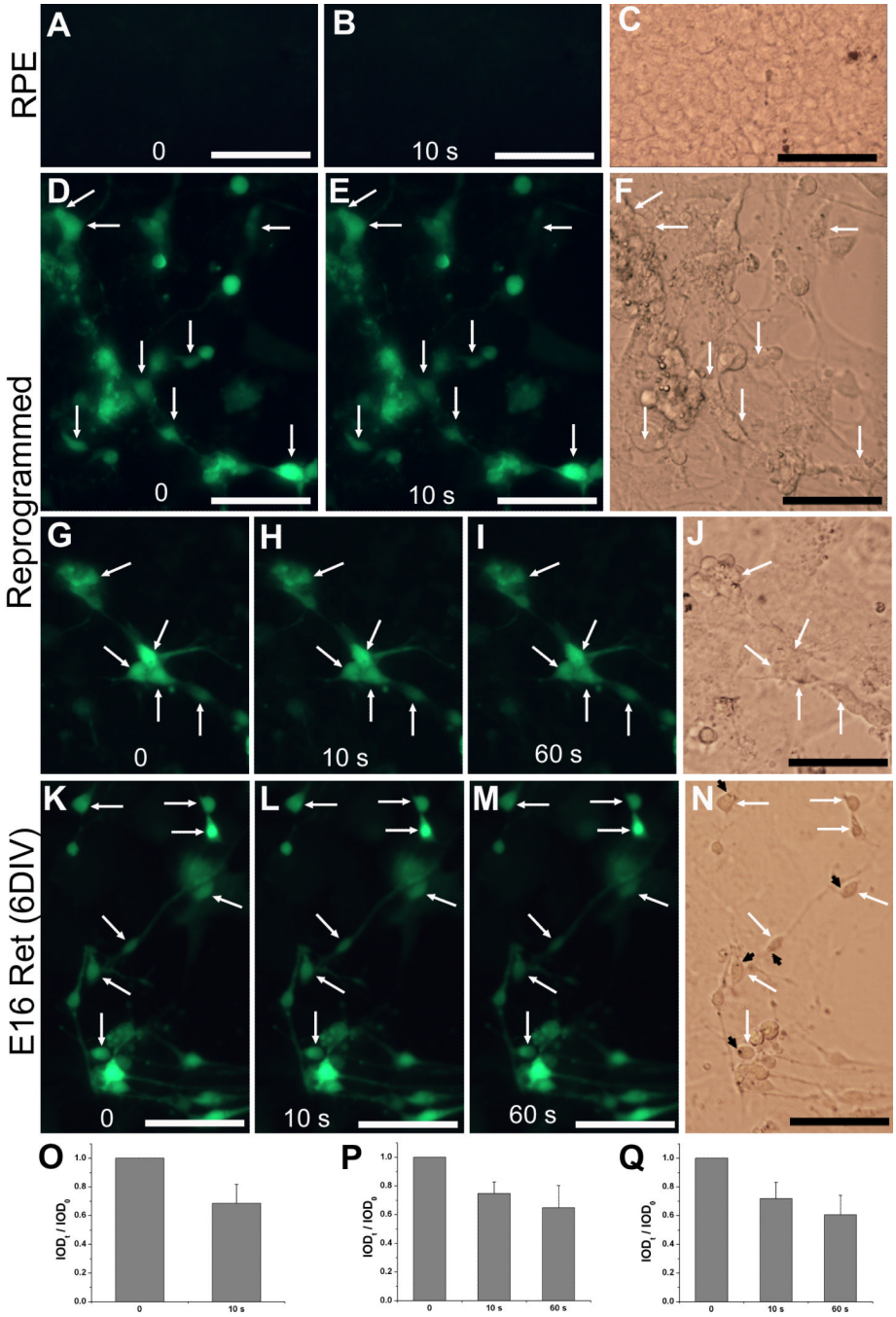

Fig. 7.

Light responses examined with Ca^{2+} imaging. A-C: Images before (A) and after 10 seconds (10 s, B) of light exposure of a control RPE cell culture infected with RCAS. D-J: Images of RPE cell cultures infected with RCAS-ngn1 before (D,G) and after 10 seconds (E,H) and 60 seconds (I) of light exposure. K-N: Images of E16 chick retinal cells after 6 days in culture [E16 Ret (6DIV)]. C,F,J,N: Bright field images. Arrows: cells with noticeable reductions in fluorescence intensities. Arrowheads: lipid-droplet-like structures. O-Q: Calculated IOD ratios (IOD_t / IOD_0) shown as means and SDs of 13-15 cells including those within the image of D,E, G-I, K-M, respectively. Scale bars: 50 μm.

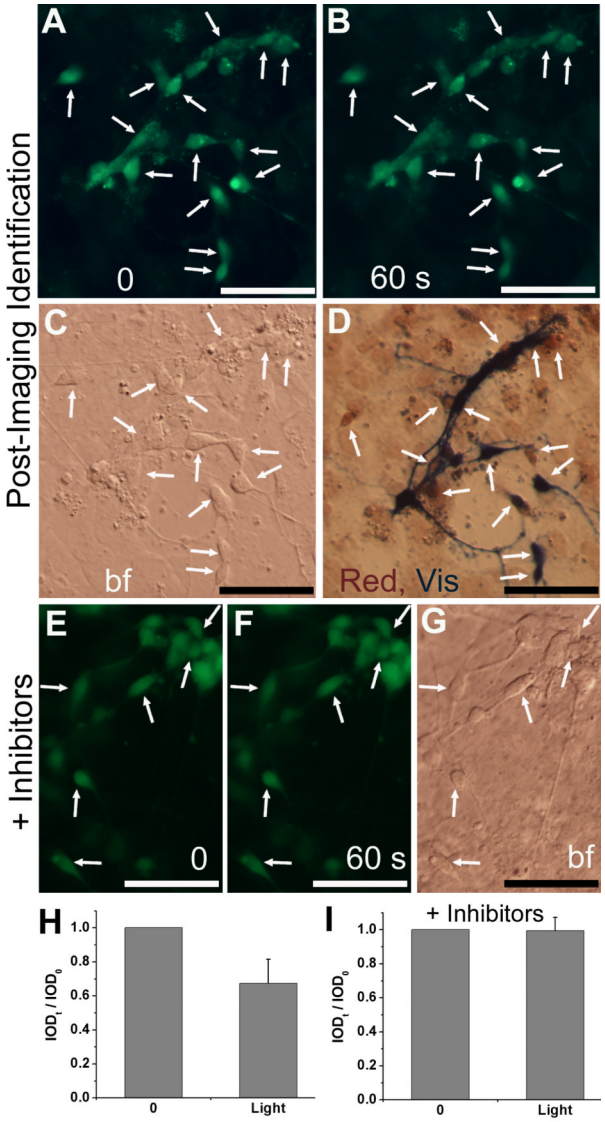

Fig. 8.

Post-Ca^{2+} imaging immunostaining and effect of CNG channel blockers on light response. A-D: Double immunocytochemistry with antibodies against red opsin and visinin post Ca^{2+} imaging. Shown are images before (A) and after 60 seconds (B) of light exposure, a bright field view (C), and after double-immunostaining (D). Arrows point to cells with noticeable decreases in fluorescence intensities and positive for visinin (Vis, in blue) and/or red opsin (Red, in red). E-G: Images before (E) and after 60 seconds (F) of light exposure in the presence of CNG channel blockers dichlorobenzamil and l-cis-diltiazem (3 μM each). Arrows point to cells with photoreceptor-like morphologies and without significant reduction in their fluorescence intensities. H,I: Calculated IOD ratios (IOD_t / IOD_0) shown as means and SDs of 14 and 10 cells including those in images A,B and E,F, respectively. Scale bars: 50 μm.

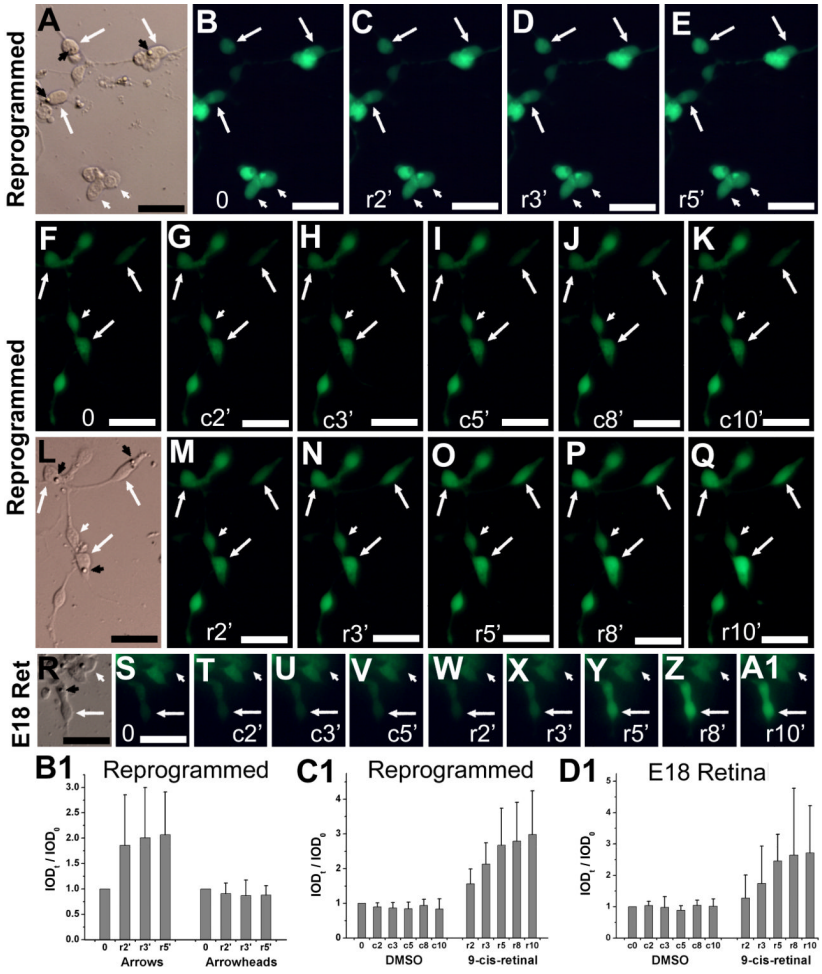

Fig. 9.

Response to 9-cis-retinal examined with Ca^{2+} imaging. A-E: Images of reprogrammed cells (in a reseeded culture) after light bleaching (B) and at 2 (C), 3 (D), and 5 (E) minutes after administration of 9-cis-retinal (r2′, r3′, r5′). F-Q: Images of reprogrammed cells after light bleaching (F) and at the indicated number of minutes (2′-10′) after sequential administration of vehicle control (c, G-K), replacement of medium (L), and then 9-cis-retinal (r, M-Q). R-A1: images of photoreceptor cells in an E18 retinal cell culture after 6 DIV. Arrows: cells showing increases in fluorescence intensity. White arrowheads: cells lacking such an increase. Black arrowheads: lipid droplet-like structure. B1-D1: The calculated IOD ratios (IOD_t / IOD_0) were shown as means and SDs of 4-8 cells from experiments B-E, F-Q, and S-A1, respectively. A,L,R: Bright field images. Scale bars: 20 μm.

Table 1

Primary antibodies used

Antigen (what is being stained for)	Immunogen (what the antibody was raised against; full sequence and species)	Manufacturer, species antibody was raised in, mono- vs. polyclonal, catalog or lot number	Dilution used
AP2; Epitope mapped to the C-terminus of human AP-2α	Human AP-2α protein	Santa Cruz Biotechnology; rabbit polyclonal; affinity purified; Cat. # SC-184	1:200
AP2α	recombinant human AP2α protein; DNA-binding domain; amino acids 208-414	Developmental Studies Hybridoma Bank (DSHB; Iowa University); mouse monoclonal; clone # 3B5; developed by Dr. T. Williams	1:50
Brn3A (Pou-domain protein)	Amino acids 186 - 224 of Brn3A fused to the T7 gene 10 protein	Chemicon/Millipore; mouse monoclonal; Cat. # MAB 1585	1:200
Calretinin	Full-length, recombinant human calretinin	Chemicon/Millipore; rabbit polyclonal; Cat. # AB 5054	1:500
Islet-1	bacterially expressed C-terminal portion of rat Islet-1; amino acids 247-349	DSHB; monoclonal; clone 39.4D5; developed by Dr. T. Jessell	1:100
LIM 1 + LIM 2	Full-length, recombinant rat LIM 2	DSHB; monoclonal; clone 4F2; developed by Dr. T. Jessell	1:50
NeuroD	The C-terminal 102 amino acids of chick NeuroD fused to the T7 phase gene 10	Our laboratory; rabbit polyclonal; affinity-purified	1:40
Opsin (red/green)	Recombinant human red/green opsin; 364 amino acids	Chemicon/Millipore; rabbit polyclonal; purified; Cat. # AB 5405	1:200
Viral p27 (27 kDa viral protein)	Purified 27 kDa virion protein extracted from avian myeloblastosis virus	Spafas; rabbit polyclonal; purified IgG; Cat. # 563301	1:500
Pax6	Recombinant chick Pax6 protein (amino acids 1 - 233)	DSHB; monoclonal; clone Pax6; developed by Dr. A. Kawakami	1:100
A 140 kDa microtubule associated protein of long-projecting axons	E10 chick tectal homogenate	Steven McLoon (University of Minnesota); monoclonal; Clone RA4	1:1,000
Vimentin (52 kDa)	E10 chick optic nerve	DSHB; monoclonal; clone H5; developed by Dr. J. Sanes	1:500
Visinin	27 kDa visinin purified from bovine eye	DSHB; monoclonal; clone 7G4; developed by Dr. C. Cepko	1:500

Table 2

Calculated numbers (per 242 mm^2) of cells expressing retinal neural markers of RPE cell cultures infected with RCAS-ngn1

Marker	Specificity	Number	% Visinin
NeuroD	Pr	271,752±38,834	89.6
crx	Pr	58,887±8,499	19.4
raxL	Pr	39,849±10,225	13.1
RXRγ	Pr	5,163±1,477	1.7
Visinin	Pr	303,307±48,722	100.0
Red opsin	Pr	4,880±2,059	1.6
cngA1/A3	Pr	968±320	0.3
alt	Pr	645±185	0.2
Calretinin	Gc, Am, Hz	5,203±960	1.7
RA4	Gc	524±185	0.2
Islet-1	Gc, Bi	-[1]	
Brn3A Gc		-	
AP2α	Am, Hz	-	
Pax6	Prg, Gc, Am	-	
LIM	Hz	-	
Vimentin	Prg, Mg	645±202	0.2

[1] negative. Gc: ganglion cells; Am: amacrine; Bi: bipolar; Hz: horizontal; Pr: photoreceptor; Prog: progenitor. Regular typeface, immunostaining; Italic, in situ hybridization.